PUBLICATION VI

Post-experimental analysis of a SOFC stack using hybrid seals

Journal of Power Sources. Elsevier.
Vol. 274 (2015), 1009–1015.

Journal of Power Sources 274 (2015) 1009–1015

Contents lists available at ScienceDirect

Journal of Power Sources

journal homepage: www.elsevier.com/locate/jpowsour

Post-experimental analysis of a solid oxide fuel cell stack using hybrid seals

O. Thomann*, M. Rautanen, O. Himanen, J. Tallgren, J. Kiviaho

VTT Technical Research Centre of Finland, P.O. Box 1000, Biologinkuja 5, Espoo, FI-02044 VTT, Finland

HIGHLIGHTS

- Post-experimental analysis of a SOFC stack after 1800 h of operation.
- Microstructural analysis of the glass-coated hybrid seal.
- Materials interactions between glass-coated seals and Crofer 22 APU interconnects.
- Dual exposure of 0.2 mm thin Crofer 22 APU plates in stack operating conditions.

ARTICLE INFO

Article history:
Received 28 July 2014
Received in revised form
8 October 2014
Accepted 16 October 2014
Available online 23 October 2014

Keywords:
SOFC
Seal
Thermiculite 866
Dual exposure
Interconnect
Post-experimental analysis

ABSTRACT

A post-experimental analysis of a SOFC stack is presented. The stack was operated for 1800 h at 700 °C with air and hydrogen and contained hybrid glass-Thermiculite 866 seals. The goal of this work was to investigate the sealing microstructure and possible corrosion during mid-term operation. It was found that hybrid seals could effectively compensate for manufacturing tolerances of cells and other components due to the compliance of the glass layer. Additionally, different interfaces were investigated for corrosion. Corrosion was not observed at two-phase interfaces such as Crofer 22 APU/glass, glass/electrolyte and glass/Thermiculite 866. The three-phase interface between Crofer 22 APU/glass/hydrogen exhibited no corrosion. Some evidence of non-systematic corrosion was found at the Crofer 22 APU/glass/air interface. The possible reasons for the corrosion are discussed. Lastly, dual exposure to humid hydrogen and air of the 0.2 mm Crofer 22 APU interconnect had no detrimental effect on the corrosion compared to air exposure. Overall the hybrid seals used in combination with the thin interconnects were found to be a promising solution due to the low leak rate and limited material interactions.

1. Introduction

Currently, key challenges for successful commercialization of SOFC are to extend their lifetime and to reduce their cost. To achieve that, effective sealing solutions that address all the seals requirements are paramount [1,2]. Seals need to withstand simultaneous exposure to the air side and to the fuel side at temperature between 650 and 850 °C. In addition, they should withstand hundreds to thousands of thermal cycles for stationary and mobile applications respectively. Additionally, seal materials should be chemically compatible with the adjacent components like metallic interconnects and cell materials. Their electrical resistivity should also be high and stable. Lastly, the seals should also be inexpensive, easy to assemble and have to compensate for manufacturing tolerances of the other stack components. Presently, glass ceramic seals are widely used in SOFC stacks. Because they are rigidly bonded to the adjacent surfaces, their coefficient of thermal expansion needs to match closely the one of the neighbouring components. They exhibit very low leak rates [3] but can be prone to degradation with thermal cycling [4]. Compressible seals composed of mica-type paper have been investigated as an alternative [5–7]. The drawback of compressive seals is that in order to achieve acceptable leak rate, a compression stress of the order of several MPa has to be applied on the stack [5]. However, it was found that the leak rate remains significantly higher compared to glass ceramic seals and that the needed level of compression and the necessary compression system becomes technically challenging for large footprint stack. These inherent issues can be addressed by adding compliant layers of glass or metal on both sides of a compressible seal [3,8,9]. The compliant layers block the main leak

* Corresponding author. Tel.: +358 401247497.
E-mail address: olivier.thomann@vtt.fi (O. Thomann).

http://dx.doi.org/10.1016/j.jpowsour.2014.10.100
0378-7753/

path between the seal and the interconnects which leads to a leakage reduction of up to 90% [9]. Additionally, Rautanen et al. showed that a compression stress as low as 0.1 MPa can be used with hybrid seals [9].

Sealing material interaction studies have been previously published but most of the articles have been focusing on glass ceramic seals interaction. Batfalsky et al. performed post-experimental investigation on stacks that had undergone rapid performance degradation [10]. They found that the interconnects had so severely corroded in the vicinity of the glass ceramic seals that the corrosion product had formed electrical bridges between adjacent interconnects and caused short-circuiting after 200 h at 800 °C. They attributed the accelerated corrosion to the presence of PbO in the glass. Menzler et al. presented results of post-experimental investigation of a stack operated for 6400 h at 800 °C [11]. They showed that the corrosion of the interconnects was enhanced in the vicinity of the glass ceramic seals but that the extent of corrosion did not compromise the performance of the stack. Wiener et al. studied interactions between Thermiculite 866 materials (a composite of vermiculite and steatite [12]) and Crofer 22 APU at 800 °C in ex situ experiments [13]. They found that the Crofer 22 APU underwent accelerated corrosion and this was attributed to the decomposition of steatite at 800 °C and transport of Mg to the oxide layer. Bram et al. studied interaction of Thermiculite 866 with Crofer 22 APU in Ref. [14]. They found that the break-away corrosion of Crofer 22 APU took place at temperature as low as 600 °C in ex situ test. They attributed the accelerated corrosion due to the steam emitted by the Thermiculite 866 during heat-up. They found that such a corrosion reaction could be prevented by a pre-oxidation treatment of the interconnects. Interestingly, corrosion was most often found at the three-phase boundary between seal material, interconnect and gas (air or fuel) [10,11,13,14]. Only few material interactions studies have been published on hybrid seals. Chou et al. studied long-term interaction of hybrid seal materials in ex situ experiments [15]. They found that the phlogopite paper was reacting with the glass they used after 500 h at 800 °C, which compromised the performance of the seal during thermal cycling. Interactions between seal materials and ferritic stainless steel were not discussed in that paper. Chou et al. published the results of a post-experimental analysis of a 3-cell stack using hybrid seals operated at 800 °C [16]. They concluded that material interaction was limited and that their material selection for the seal and interconnect material was suitable for long-term operation. However, the three-phase interfaces between seal/interconnect/gases were not discussed.

Dual atmosphere exposure of interconnects has also drawn some attention in the literature. Skilbred et al. and Yang et al. studied the effect of dual atmosphere exposure at 800 and 850 °C on the corrosion of Fe–Cr–Mn steels and they showed that dual exposure affects the oxide scale composition with a higher concentration of Fe in the oxide scale on the air side. Exposure time was limited to 500 h and 300 h [17–19]. Holcomb et al. studied dual exposure of the austenitic steel 316L and found that heavy corrosion was taking place after 100 h at 700 °C. It was caused by the diffusion of oxygen and hydrogen in the alloy and the formation of steam in the metal alloy near the oxide layer, which formed a thick and porous oxide layer [20].

The amount of data available on dual exposure of interconnect steels is presently limited, which is partly explained by the fact that dual exposure tests are more complex than single atmosphere exposure tests. Additionally, the durations of the experiments are typically in the few hundred hours range. The hydrogen atmosphere is often lean with 5% hydrogen in argon for safety reason and the humidity restricted to 3%, whereas these values are typically higher inside a stack.

The thickness of the interconnects is also affecting their lifetime by decreasing the initial reservoir of Cr. Stainless steel alloys are protected from excessive corrosion by the formation of a Cr oxide layer. During operation, the Cr from the protective scale evaporates and is replaced by Cr diffusing from the bulk of the alloy. The Cr is consumed until it reaches a concentration of about 16% in the alloy, when break-away oxidation start to occur [21]. On the one hand, it is interesting to reduce interconnect thickness to reduce the cost associated with the interconnect steel, but on the other hand Asensio-Jimenez et al. showed that the corrosion rate of interconnect steel increases for thinner plate thickness [22]. Therefore data on the corrosion of thin interconnect are valuable.

This present paper contributes to the field with the results of the post-experimental analysis of a SOFC stack using hybrid seal consisting of a Thermiculite 866 compressible core with compliant glass layers. The seal cross-section has been extracted from a single-cell stack that was operated for 1800 h at 700 °C. The in situ nature of the experiment provides exposure conditions to the seals and interconnects that are closer to stack operation compared to ex situ experiments. For example, the steam content in this work was 20% at anode outlet, which is higher compared to ex situ seals (usually maximum 3%). However, even higher steam content is expected in a stack in an actual system environment (from 60 to 80% steam content).

The goals of the post-experimental analysis were: i) to investigate the microstructure of the hybrid seals, ii) to evaluate material interactions between the seal materials and the interconnects and iii) to investigate the effect of dual exposure on thin 0.2 mm interconnects. The stack presented here is a stack prototype developed at VTT Technical Research Centre of Finland in which hybrid seals were used. After this work, the hybrid seal design has been significantly improved by a 10-fold reduction of the amount of glass and the cost associated to it [9].

2. Experimental

The single cell stack used a co-flow configuration. Crofer 22 APU (ThyssenKrupp, Germany) was used for interconnects and end-plates. The interconnects were 0.2 mm in thickness. The anode-supported cell was manufactured by Elcogen AS (Estonia) and is 10×10 cm^2. Hybrid seals were used for all seals located between Crofer 22 APU plates and are made with consolidated Thermiculite 866 (Flexitallic LTd, the United-Kingdom) [12] between two glass tapes of 220 μm green thickness. The glass used belongs to the system MO (M = Mg, Ca)–Al_2O_3–BaO– SiO_2–B_2O_3 (GM31107, Schott, Germany [23]). The Thermiculite 866 is composed in nearly equal amount of vermiculite and steatite, which compositions are $[(K, Mg, Fe)_3(Si,Al)_4O_{10}(OH)_2]$ and $[(Mg_3Si_4(OH)_2]$ respectively. The seal between the cell electrolyte (yttria-stabilized zirconia (YSZ)) and Crofer 22 APU plate was made of glass without Thermiculite 866. 40 kg of weight was added on the stack, which corresponds to a compressive stress of ca. 0.1 MPa assuming that all the weight was carried by the seals and not by the cell.

Dry hydrogen and dry air were used as fuel and oxidant. Pure hydrogen was selected as fuel, which exposes the seals to a worst case condition as it has been shown that the leak rate through hybrid seal increases with the concentration of hydrogen [9]. The stack was operated at 700 °C for 1800 h. Average current density was 0.2 Acm^{-2} and fuel utilisation and air utilisation were 18%. The hydrogen cross leak value corresponded to a loss of 0.9% of the inlet hydrogen flow in these operating conditions, which is low. The cross leak value was calculated according to the method described in Ref. [9].

After the test, the stack was mounted in epoxy and a cross-section was extracted from the area close to the gas outlet for

SEM and EDS analysis. This area was selected because the exposure conditions are expected to be the most challenging due to the increased steam content.

Post-experimental analysis was carried out using SEM observation and energy-dispersive x-ray spectroscopy (EDS) on JSM-6400 Scanning Microscope from JEOL equipped with a Prism 2000 detector and Spirit 1.06.02 Analyzer software from Princeton Gamma-Tech (PGT). The oxide layer thickness was determined by measuring the area on the image corresponding to the oxide phase with ImageJ [24] and dividing it by the picture width according to the method described in Ref. [25].

3. Results and discussion

3.1. Glass compliance

A cross-section of two hybrid seals is illustrated in Fig. 1. It can be seen that the Thermiculite 866 material is significantly deformed by the die-cutting process forming protruding cutting burrs near the edges. Despite the unevenness of the Thermiculite 866, the glass has well accommodated the gap varying between 15 and 150 μm for the upper seal shown in Fig. 1. Pore formation took place only at the location were the Thermiculite 866 is at its thinnest, however these pores are closed and don't form a continuous leak path. Additionally, some excess glass was extruded out of the seal because of the compliance of the glass. This means that the glass tape thickness could be thinner or other methods to apply thinner glass coating could be used. Moreover, the clearances between the Crofer 22 APU plates are 710 and 580 μm at the location of measurement for the two seals shown and this difference in clearance didn't seem to have decreased the quality of the seals at these locations. This demonstrates the benefit of using hybrid seals over purely compressible seals. In short, similar hybrid seals were able to effectively seal gaps between 580 and 710 μm and the glass layer was able to compensate 140 μm thickness variation of the Thermiculite 866. Compressible seals would have required much larger compression stress to flatten the cutting burrs. Additionally, the gap clearance variation would have likely been an issue due to the limited compressibility of Thermiculite 866 [5]. There are many reasons that can lead to a variation of gap clearance in a stack, i.e. differences in cell and interconnect plate thickness, and variation of thickness of the compressible Thermiculite 866. These variations can be decreased to a certain level by more uniform manufacturing methods but cannot be totally avoided. Moreover, generally decreasing the manufacturing tolerance comes with a cost increase. It is therefore of high interest that the seals can accommodate the geometric variation in a stack.

3.2. Materials interactions between seal materials and interconnects

This section presents results of different material interactions, such as Crofer/glass, glass/Thermiculite 866 and glass/electrolyte interfaces. In addition, interactions at the three-phase interfaces such as Crofer/glass/air and Crofer/glass/hydrogen are detailed.

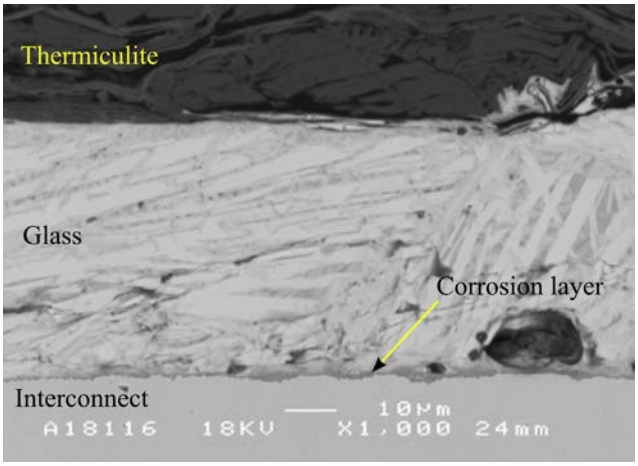

Fig. 2. SEM BSE cross-section of Crofer/glass and glass/Thermiculite 866 interfaces.

3.2.1. Crofer/glass and glass/Thermiculite 866 interfaces

The Crofer/glass and glass/Thermiculite 866 interfaces are illustrated in Fig. 2. This picture has been taken from the middle section of the seal, which means that its exposure to gas is limited to possible leakage through the seal. It appears that the materials have good chemical compatibility and only limited corrosion can be seen between glass and Crofer 22 APU with an oxide layer of less than 1 μm. As a comparison, the oxide layer thickness is thinner in contact with the glass compared to the case when the Crofer 22 APU is exposed to air at the same temperature (see results in Section 3.3). Therefore, it was concluded that the presence of glass did not accelerate the oxidation of the Crofer 22 APU plate at this interface.

3.2.2. Crofer/glass/air interface

Cross-section pictures from the Crofer/glass/air interface are illustrated in Fig. 3 and Fig. 4. The cross-section sample is taken near the air exhaust. The humidity in air downstream of the stack was measured to be ca. 0.4% during stack operation. The cracks present in the glass are due to sample preparation.

The location shown in Fig. 3(a) and (b) corresponds to the upper and lower corners of the seal which is exposed to the same cathode atmosphere, and they are therefore exposed to the same air atmosphere. However, their corrosion behaviour differed significantly. The upper side shows no sign of significant corrosion while the lower side has developed a 20 μm corrosion layer just at the location where the glass layer ends. The corrosion layer does not extend more than 200 μm from the three-phase interface. As it can be seen from the EDS analysis in Fig. 3(d), the oxide layer consists of a first layer of mixed oxide of Cr and

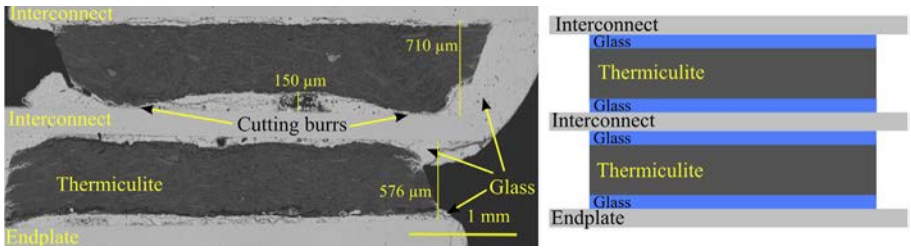

Fig. 1. SEM BSE cross-section of two frame seals. The seals are composed of a Thermiculite 866 core between two glass layers.

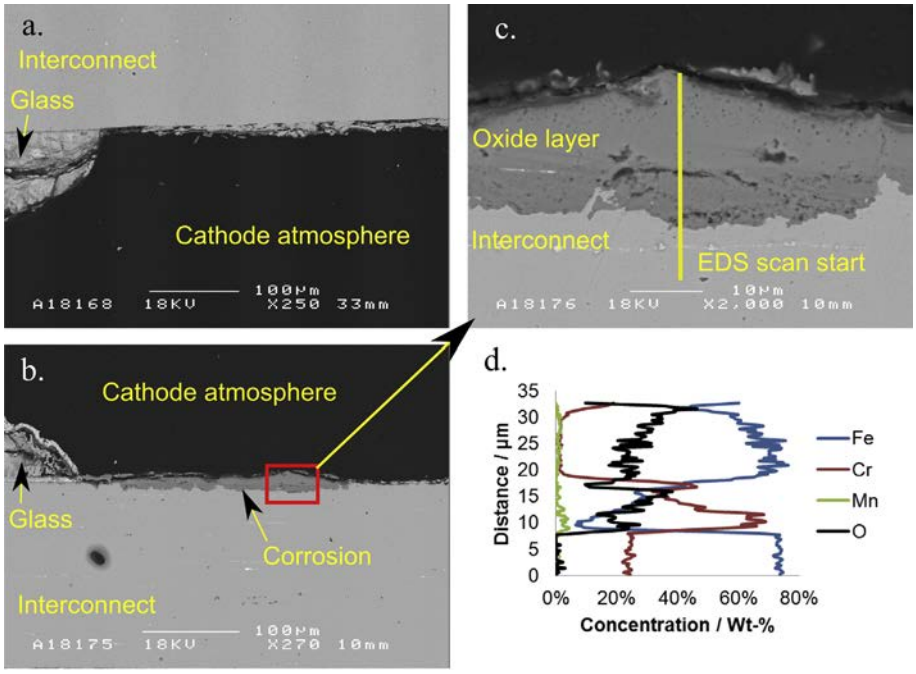

Fig. 3. SEM BSE cross-sections of two Crofer/glass/air interfaces (a and b) that are both exposed to cathode atmosphere. Magnified view of cross-section (c).

Mn and the top layer is mainly composed of Fe oxide. This is a clear example of break-away oxidation, i.e. when the Cr oxide layer cannot anymore protect the stainless steel because of too fast corrosion. It is however surprising that such extent of corrosion takes place only at one corner of the seal (Fig. 3(b)) and not at the other (Fig. 3(a)), despite the exposure condition being identical.

Similarly, pictures shown in Fig. 4(a and b) correspond to two different seals but exposed to the same atmosphere; the air exhaust manifold. Also in this case, no significant corrosion takes place at one side (Fig. 4(a)) and break-away oxidation took place at the other side (Fig. 4(b)), where the oxide layer is 20 µm thick. Accelerated corrosion was found to extend millimetres away from the seals into the air manifold towards the stack air outlet. The oxide layer was thicker 5 mm away from the seal, where it was about 120 µm thick and its top layer was composed mainly of Fe oxide (picture not shown). However, corrosion in the manifold of the thick end plate is not critical for the stack performance.

Different reasons can have caused the Crofer 22 APU to undergo break-away oxidation at some locations. Cr evaporation from the oxide layer is enhanced by the presence of water vapour in air [26,27] and if the evaporation rate of Cr is higher than the rate at which the Cr oxide layer is formed, the stainless steel undergoes break-away oxidation. It is possible that the steam content was locally higher where the break-away oxidation took place. Steam content can be locally higher in case there is a local leak of hydrogen. However this does not appear to be the case here because the seals shown in Figs. 3 and 4 are exposed to air on both sides. The heavy corrosion found deep in the air manifold could be attributed to the presence of contamination from lubricant used during machining of the manifolds. The endplates were heat-treated after machining (800 °C for 12 h) during which possible lubricant was burned, then the plates were polished and then cleaned in laboratory glassware washer and by wiping with ethanol impregnated tissues before use but it is difficult to remove lubricant or burned lubricant residues from the narrow manifolds. This hypothesis is supported by the fact that the heaviest corrosion was found deep in the manifold, several millimetres away from the seal. Lastly, it cannot be excluded that the corrosion could be caused by element evaporating from the glass or Thermiculite 866. Both are made of complex elemental formulations and have potentially many candidates for evaporation and subsequent interactions.

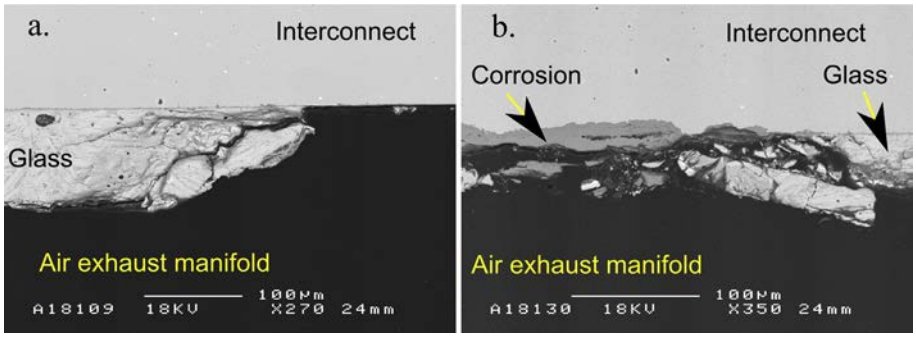

Fig. 4. SEM BSE cross-sections of two Crofer/glass/air interfaces (a and b) that are both exposed to the atmosphere of the air exhaust manifold.

However, if the corrosion mechanism would be from material interaction, one would expect it to happen systematically, which is not the case here.

Bram et al. found similar corrosion behaviour of Crofer 22 APU in their paper on material interactions between Thermiculite 866 and Crofer 22 APU [14]. In their work, they exposed Thermiculite 866 (without any glass) to air and dual atmosphere at 600 °C for 400 h and found that break-away oxidation was taking place at the air side. They attributed the corrosion behaviour of the Crofer 22 APU to the enhanced water concentration near the seal that was originating from vermiculite dehydration and steatite decomposition. This phenomenon was previously described and quantified by Wiener et al. [13]. According to Bram et al., the break-away oxidation behaviour can be suppressed by pre-oxidation of the interconnect plates.

The reason for the accelerated corrosion at the air side remains unclear and is the subject of further research. The main risk associated with the accelerated corrosion found near the seals is the formation of porous Fe oxide all the way through the 0.2 mm thin interconnects and creation of a leak path through the interconnect. Secondarily, in extreme case, accelerated corrosion can form a lump of electrically conductive Fe oxide and creates short-circuiting by connecting adjacent interconnect plates [10]. However, it appears that the corrosion is limited after 1800 h and didn't spread far towards the cathode, therefore it is unlikely that the growth of the oxide layer would affect the area-specific resistance of the interconnect. The most corroded locations were found in the air exhaust manifold on the 2 cm-thick end plate where accelerated corrosion has no consequence for the stack performance. Lastly, it is interesting to notice that corrosion took place near the three-phase boundary and not at the glass/metal (two-phase) interface, which is coherent with findings of several previous studies [10,11,13,14]. As mentioned, dry air was used during the test. In order to subject the materials on the cathode side to a more challenging atmosphere, pre-humidified air (e.g. 1 … 3%) could be used to see the effect of humid air on material corrosion.

3.2.3. Crofer/glass/humid hydrogen interface

A micrograph from the Crofer/glass/humid hydrogen interface is shown in Fig. 5. No significant material interaction could be seen at the interface between seal and humid hydrogen. The humidity of the fuel is also at its highest at this location, about 20%, due to water production from reaction at anode. The cracks in the glass are due to sample preparation.

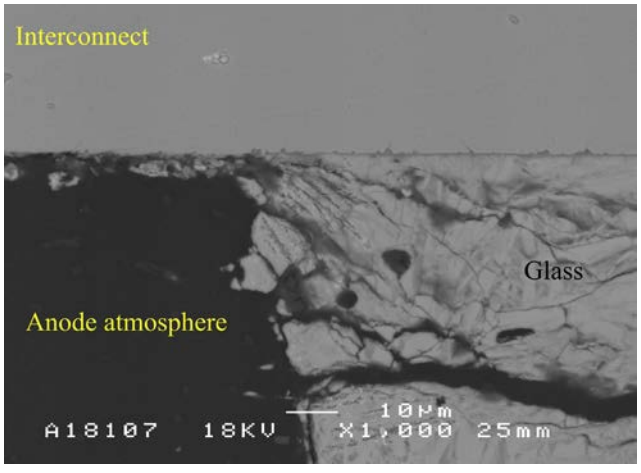

Fig. 5. SEM BSE cross-section at the Crofer/glass/humid hydrogen interface. The visible glass is part of the cell seal which is composed of glass without any Thermiculite 866.

3.2.4. Glass/electrolyte interface

The glass/electrolyte interface is illustrated in Fig. 6. The glass contains little porosity and exhibits a good adherence to the YSZ of the electrolyte. There is no evidence of corrosion between the electrolyte and the glass.

3.3. Corrosion of interconnects exposed to dual atmosphere

The post-experimental analysis of this stack also offers valuable insight into the corrosion of thin interconnects in dual atmosphere compared to exposure to single air atmosphere.

Fig. 7(a and b) show cross-sections from the interconnect plate exposed simultaneously to air and humid hydrogen. The location is near the fuel exhaust and the absolute humidity in the fuel atmosphere was about 20%. Fig. 7(c and d) show cross-sections from an interconnect exposed to air atmosphere on both side. On Fig. 7(a), a crack from sample preparation is present in the oxide layer, splitting it into two layers.

For the single air exposure case shown in Fig. 7(c and d), the oxide layers were 1.4 μm and 1.9 μm in thickness. In case of dual exposure, the oxide layers were found to be of 1.3 μm and 1.2 μm in thickness (Fig. 7(a and b)). The EDS scans suggest that the oxide layer formed in dual exposure is rich in Cr and Mn oxide at both sides. The morphology of the oxide layer depends on the conditions of exposure with a tendency for the oxide layer formed in air to be smoother than the one formed in fuel atmosphere. It was previously shown in the literature that the spinel crystals growing on the surface of ferritic Fe–Cr–Mn steel were dependant on the atmosphere composition [28]. Some limited inwards growth of surface oxide can be seen in Fig. 7(a, b and c) but limited to a depth of 5 μm from the metal surface. It is difficult to find comparable oxide layer thickness data from the literature due to the numerous conditions to be taken into account (temperature, time and atmosphere composition). Linder et al. found that Crofer 22 APU oxide layer thickness was about 5 μm for similar exposure time at 850 °C in air [25]. Sachitanand et al. found that Crofer 22 APU oxide layer thickness was about 12–16 μm at 850 °C in humidified air after 1000 h [29].

The results presented in Fig. 7 lead to three main findings. Firstly, the oxide layers are thin for interconnect without protective coating, showing that the selected interconnect alloy exhibits suitable corrosion-resistance at an operating temperature of 700 °C. Additionally, dual exposure had no detrimental effect on the corrosion rate of the interconnect and the oxide layers were actually thinner in the dual exposure case compared to exposure to air only. Lastly, the interconnect thickness used for this stack (0.2 mm) is relatively thin and therefore the reservoir of Cr in the bulk steel is limited. However, it appears that the low thickness of the interconnects had no significant detrimental effect on their corrosion rate.

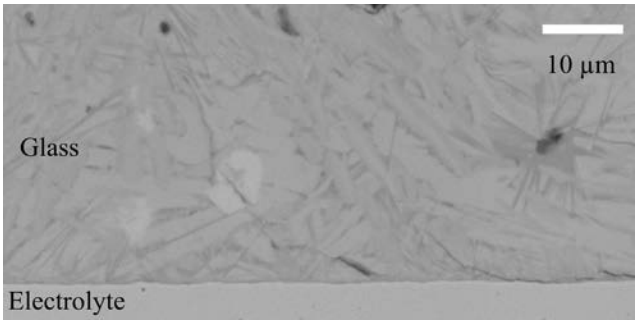

Fig. 6. SEM BSE cross-section at the interface between glass and electrolyte.

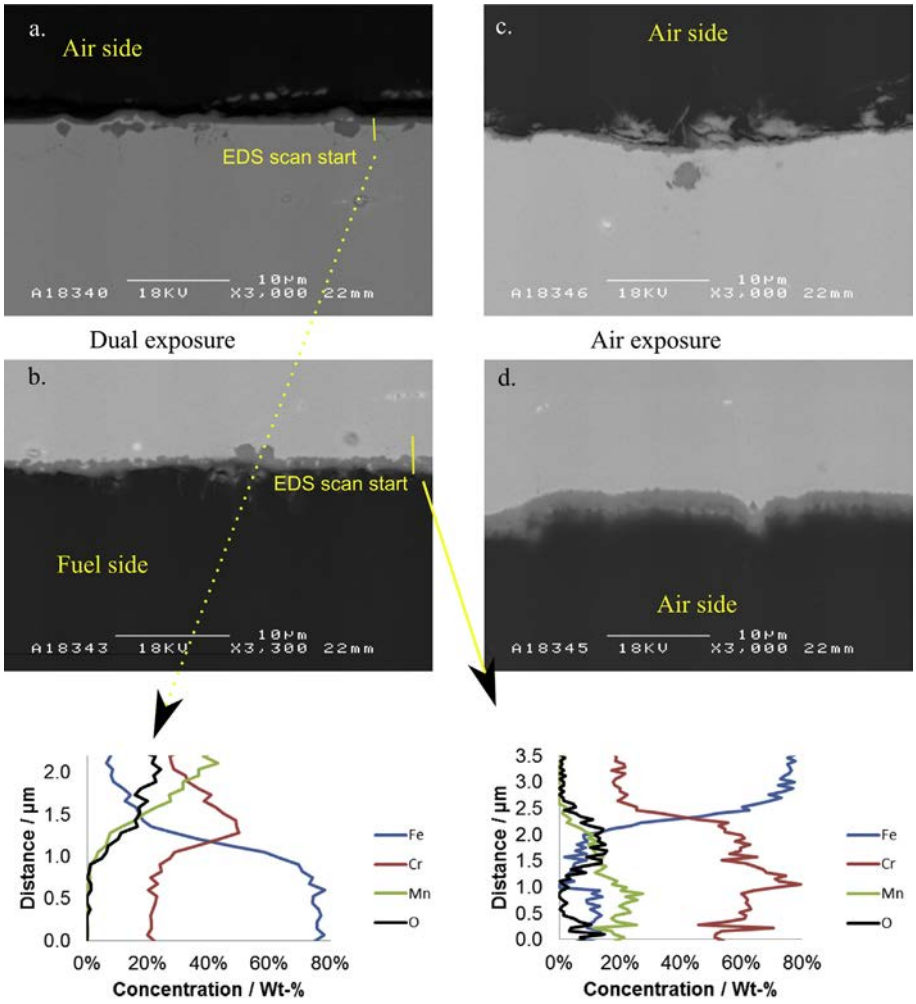

Fig. 7. SEM BSE cross-sections of a 0.2 mm thin interconnect plate exposed simultaneously to air and humid hydrogen (a and b) with two EDS scan. Another interconnect exposed to air on both side (c and d).

4. Conclusions

In this article, post-experimental analysis results of a single-cell stack containing hybrid seals are detailed. The hybrid seal solution was found to work well because it could successfully compensate for thickness variation of stack element of about 150 μm. In addition, the compliant glass layer could well accommodate the unevenness of the Thermiculite 866 caused by the die-cutting process. The hydrogen cross leak value corresponded to a loss of 0.9% of the inlet hydrogen flow, which is very low. Different interfaces and locations inside the stack were investigated for corrosion. Corrosion didn't take place at two-phase interfaces such as Crofer/glass, glass/electrolyte and glass/Thermiculite 866. The three-phase interface between Crofer/glass/hydrogen exhibited no corrosion, whereas some of the locations corresponding to the Crofer/glass/air interface exhibited some non-systematic corrosion. The possible reasons for the corrosion found were discussed and the most likely reason for corrosion is contamination from lubricant that was not properly removed before stack assembly. These results will be the basis of a future study on the corrosion of Crofer 22 APU in contact with sealing materials ex situ, which will aim at improving our understanding of this phenomenon. Lastly, dual exposure of thin Crofer 22 APU interconnect did not cause enhanced corrosion compared to air exposure and the oxide layer thickness was found to be limited below 2 μm. Overall the hybrid seals used in combination with the thin interconnects were found to be a promising solution due to low leak rate and its suitability for long-term operation will be examined further in stack operated for longer period of time.

Acknowledgements

Finnish Funding Agency for Technology and Innovation (TEKES) is acknowledged for financial support. Seija Kivi from VTT is acknowledged for sample preparation, Kai Nurminen, Kari Koskela from VTT and Jorma Stick from SataHitsaus are acknowledged for the experimental part of the work. Risto Parikka from VTT Expert Services Oy is acknowledged for SEM analysis.

References

[1] J.W. Fergus, J. Power Sources 147 (2005) 46–57.
[2] K. Weil, JOM 58 (2006) 37–44.
[3] Y.-S. Chou, J.W. Stevenson, L.A. Chick, J. Power Sources 112 (2002) 130–136.
[4] R.N. Singh, Int. J. Appl. Ceram. Technol. 4 (2007) 134–144.
[5] M. Rautanen, O. Himanen, V. Saarinen, J. Kiviaho, Fuel Cells 9 (2009) 753–759.

[6] Z. Wuillemin, N. Autissier, M. Nakajo, M. Luong, J. Van Herle, D. Favrat, J. Fuel Cell Sci. Technol. 5 (2008).
[7] S.P. Simner, J.W. Stevenson, J. Power Sources 102 (2001) 310–316.
[8] Y.-S. Chou, J.W. Stevenson, L.A. Chick, J. Am. Ceram. Soc. 86 (2003) 1003–1007.
[9] M. Rautanen, O. Thomann, O. Himanen, J. Tallgren, J. Kiviaho, J. Power Sources 247 (2014) 243–248.
[10] P. Batfalsky, V.A.C. Haanappel, J. Malzbender, N.H. Menzler, V. Shemet, I.C. Vinke, R.W. Steinbrech, J. Power Sources 155 (2006) 128–137.
[11] N.H. Menzler, P. Batfalsky, L. Blum, M. Bram, S.M. Groß, V.A.C. Haanappel, J. Malzbender, V. Shemet, R.W. Steinbrech, I. Vinke, Fuel Cells 7 (2007) 356–363.
[12] J.R. Hoyes, S. Bond, Sealing Technol. (2007) 11–14.
[13] F. Wiener, M. Bram, H. Buchkremer, D. Sebold, J. Mater. Sci. 42 (2007) 2643–2651.
[14] M. Bram, L. Niewolak, N. Shah, D. Sebold, H.P. Buchkremer, J. Power Sources 196 (2011) 5889–5896.
[15] Y.-S. Chou, J.W. Stevenson, J. Hardy, P. Singh, J. Power Sources 157 (2006) 260–270.
[16] Y.-S. Chou, J.W. Stevenson, J.-P. Choi, J. Power Sources 250 (2014) 166–173.
[17] Z. Yang, G. Xia, M.S. Walker, C. Wang, J.W. Stevenson, P. Singh, Int. J. Hydrogen Energy 32 (2007) 3770–3777.
[18] B. Skilbred, A. Werner, H. Reidar, Int. J. Hydrogen Energy 37 (2012) 8095–8101.
[19] Z. Yang, M.S. Walker, P. Singh, J.W. Stevenson, T. Norby, J. Electrochem.Soc. 151 (2004).
[20] G.R. Holcomb, M. Ziomek-Horoz, S.D. Cramer, B.S. Covino Jr., S.J. Bullard, J. Mater. Eng. Perform. 15 (2006) 404–409.
[21] P. Huczkowski, V. Shemet, J. Piron-Abellan, L. Singheiser, W.J. Quadakkers, N. Christiansen, Mater. Corros. 55 (2004) 825–830.
[22] C. Asensio-Jimenez, L. Niewolak, H. Hattendorf, B. Kuhn, P. Huczkowski, L. Singheiser, W.J. Quadakkers, Oxid. Met. 79 (2013) 15–28.
[23] D. Goedeke, J. Besinger, Y. Pfluegler, B. Ruedinger, ECS Trans. 25 (2009) 1483.
[24] M.D. Abràmoff, P.J. Magalhães, S.J. Ram, Biophoton. Int. 11 (2004) 36–42.
[25] M. Linder, T. Hocker, L. Holzer, K.A. Friedrich, B. Iwanschitz, A. Mai, J.A. Schuler, J. Power Sources 243 (2013) 508–518.
[26] C. Gindorf, L. Singheiser, K. Hilpert, J. Phys. Chem. Solids 66 (2005) 384–387.
[27] O. Thomann, M. Pihlatie, J.A. Schuler, O. Himanen, J. Kiviaho, Electrochem. Solid State Lett. 15 (2012) B35–B37.
[28] Z. Yang, J.S. Hardy, M.S. Walker, G. Xia, S.P. Simner, J.W. Stevenson, J.Electrochem.Soc. 151 (2004) A1825–A1831.
[29] R. Sachitanand, M. Sattari, J. Svensson, J. Froitzheim, Int. J. Hydrogen Energy 38 (2013) 15328–15334.